Stony Brook University

Characterization of Disease Related Missense Mutations in Vacuolar Sorting Protein 13 of *Saccharomyces Cerevisiae*

A Thesis Presented

by

Robert Anthony Policastro

to

The Graduate School

in Partial Fulfillment of the

Requirements

for the Degree of

Master of Science

in

Biochemistry and Cell Biology

Stony Brook University

December 2014

Stony Brook University

The Graduate School

Robert Anthony Policastro

We, the thesis committee for the above candidate for the

Master of Science degree, hereby recommend

acceptance of this thesis.

Aaron Neiman, Ph.D.
Professor, Biochemistry and Cell Biology

Sasha Levy, Ph.D.
Assistant Professor, Biochemistry and Cell Biology

This thesis is accepted by the Graduate School

Charles Taber
Dean of the Graduate School

Abstract of the Thesis

Characterization of Disease Related Missense Mutations in Vacuolar Sorting Protein 13 of *Saccharomyces Cerevisiae*

by

Robert Anthony Policastro

Master of Science

in

Biochemistry and Cell Biology

Stony Brook University

2014

Vps13 is a large evolutionarily conserved protein of 3144 amino acids found in *S. cerevisiae*. Vps13 has been connected to disparate roles in the cell, including the retention of proteins in the trans golgi network, proper phospholipid composition and closure of the prospore membrane during sporulation, and a genetic interaction with the ERMES complex which brings the ER and mitochondria to close proximity. Mutations in *VPS13A*, a *VPS13* ortholog found in humans, has been linked to a late onset neurodegenerative disease similar to Huntington's disease, called chorea acanthocytosis (ChAc). Previous sequencing of *VPS13A* in some ChAc patients uncovered missense mutations, which may provide insight into which role(s) of Vps13A are linked to the disease symptoms of ChAc. Of these missense mutations, we found three with clear cognate residues in Vps13 through Blastp alignment. This has allowed us to engineer these missense mutations into *S. cerevisiae* using a CRISPR/Cas9 method so that assays could be run to look potential defects. These assays include western blot analysis of carboxypeptidase Y sorting to check for TGN retention of Vps10, lethality in combination with *mmm1*Δ (a member of the ERMES complex), and the ability to form spores after being crossed to a strain containing *vps13*Δ and being

plated on a media that induces sporulation. These assays have uncovered that two of the missense mutants, *vps13-L66P* and *vps13-Y2702C*, are lethal in combination with *mmm1*Δ. Amongst other functions, phospholipid exchange between the ER and mitochondria is an important process at the ER-mitochondrial junction, of which Mmm1 and the ERMES complex maintains. These results suggest that Vps13 and its ortholog Vps13A are potentially important for proper phospholipid exchange to the mitochondria through a yet unknown interaction at the ER-mitochondrial junction, and that this may be the cause of the disease symptoms in ChAc.

Table of Contents

Figures

Tables

Abbreviations

5-FOA	5-Fluoroorotic acid
Cas9	CRISPR Associated Protein 9
ChAc	Chorea Acanthocytosis
CPY	Carboxypeptidase Y
CRISPR	Clustered Regularly Interspaced Short Palindromic Repeats
DNA	Deoxyribonucleic Acid
DPAP-A	Dipeptidyl Aminopeptidase A
DUF1162	Domain of Unknown Function 1162
EDTA	Ethylenediaminetetraacetic acid
EPB41	Erythrocyte Membrane Protein Band 4.1
ER	Endoplasmic Reticulum
ERMES	ER-mitochondria Encounter Structure
G418	Geneticin
GEM1	GTPase EF-hand Protein of Mitochondria
GTPase	Guanosine-5'-triphosphatease
KanR	Kanamycin Resistance
KEX2	Killer Expression defective
LiAc	Lithium Acetate
MDM10	Mitochondrial Distribution and Morphology 10
MDM12	Mitochondrial Distribution and Morphology 12
MDM34	Mitochondrial Distribution and Morphology 34
MMM1	Maintenance of Mitochondrial Morphology
PCR	Polymerase Chain Reaction
PDH	Pyruvate Dehydrogenase
$PI(4,5)P_2$	Phosphatidylinositol 4,5-bisphosphate
PSM	Prospore Membrane
PVDF	Polyvinylidene fluoride
RNA	Ribonucleic Acid
SAM_{holo}	Sorting and Assembly Machinery Holo Complex

SDS	Sodium dodecyl sulfate
SPO14	Sporulation 14
SPO71	Sporulation 71
TCA	Trichloroacetic Acid
TGN	Trans-Golgi Network
vCLAMP	Vacuole and Mitochondria Patch
VPS10	Vacuolar Protein Sorting 10
VPS13	Vacuolar Protein Sorting 13
VPS13A	Vacuolar Protein Sorting 13A
VPS39	Vacuolar Protein Sorting 39
YPD	Yeast Extract Peptone Dextrose
YPT7	Yeast Protein Two 7

I. Introduction

1. Introduction to *VPS13*

Vps13 is a large, highly conserved protein encoded by *VPS13* in *Saccharomyces cerevisiae* that has been implicated in multiple cell processes. *VPS13* orthologs are ubiquitous in many eukaryotic genomes, including humans (Rampoldi et al., 2001). In *S. cerevisiae*, Vps13 is 3144 amino acids, and has two named domains and two additional regions of high conservation. The first 100 amino acids of the N-terminus comprise the N-chorein domain, which does not have a known function (Velayos-Baeza et al., 2004, Hayashi et al., 2012). A second domain of unknown function, DUF1162, extends between amino acids 2200 and 2500 (Hayashi et al., 2012, Velayos-Baeza et al., 2004). Between amino acids 650 and 1300 is a region of conservation that includes two repeat sequences (Velayos-Baeza et al., 2004), and the last 500 amino acids of the C-terminus are highly conserved (Hayashi et al., 2012, Velayos-Baeza et al., 2004). This conservation among species suggests an important role for the protein in the cell. Analysis of *VPS13* mutants in *S. cerevisiae* has provided insight on three distinct functions of the protein.

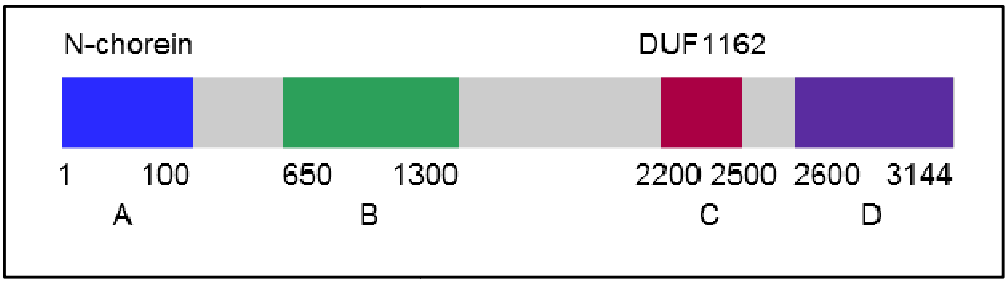

Figure 1 **Conserved regions in Vps13p of *S. cerevisiae*.**
The first 100 amino acids on the N-terminus comprise the N-chorein domain (A). Between amino acids 650 and 1300 is a region of sequence conservation (B). The DUF1162 domain resides between amino acids 2200 and 2500 (C). The last 500 amino acids on the C-terminus have high conservation (D).

The first discovered role of Vps13p in *S. cerevisiae* is in delivery of Carboxypeptidase Y (CPY), a vacuolar protease, to the vacuole (Bankaitis et al., 1986). When *VPS13* is deleted, CPY is secreted from the cell from the Trans-Golgi Network (TGN), rather than sorted for delivery to the vacuole (Robinson et al., 1988). The secreted CPY is a larger 69 kDa glycosylated precursor, which is normally cleaved and activated into its mature 61 kDa form in the vacuole (Stevens et al., 1982). The secretion of CPY out of the cell in *vps13*Δ mutants is thought to occur because of a defect in the recycling of Vps10p back to the TGN from the late endosome (Marcusson et al., 1994).

Vps13p is important for the retention of proteins in the TGN such as Vps10 and Kex2, through retrograde transport. Vps10p is a transmembrane receptor that cycles between the TGN and late endosome to sort enzymes such as CPY to the vacuole (Marcusson et al., 1994). *vps10*Δ mutants secrete the CPY precursor out of the cell, similar to *vps13*Δ mutants (Brickner and Fuller, 1997). When *VPS13* is deleted, there is a loss of Vps10p localization to the TGN, which precipitates the secretion of CPY out of the cell (Brickner and Fuller, 1997). Similar to Vps10, Kex2p is a transmembrane protease that normally cycles between the TGN and late endosome. *vps13*Δ mutants also lose localization of Kex2p to the TGN (Brickner and Fuller, 1997), which is consistent with the role of Vps13p in late endosome to TGN trafficking. This further indicates that the CPY sorting defect in *vps13*Δ mutants is indicative of a general defect in retrograde transport between the late endosome and TGN.

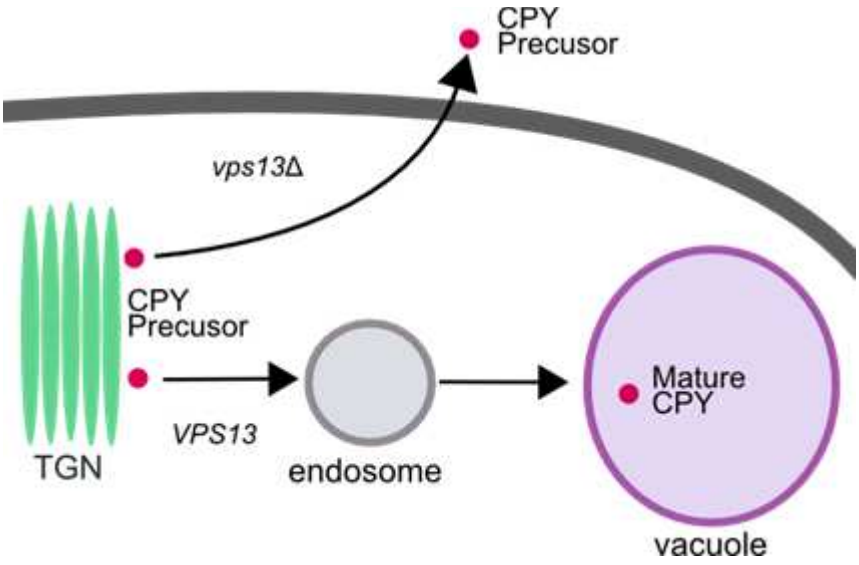

Figure 2 **CPY sorting in *S. cerevisiae* in *VPS13* and *vps13*Δ cells.**
The CPY precursor normally gets transported to the vacuole before cleavage and maturation (Bankaitis et al., 1986). In *vps13*Δ mutants the precursor form of CPY is secreted from the cell instead (Robinson et al., 1988).

1.1 **Sporulation**

Vps13p has a role in sporulation of *S. cerevisiae*. *S. cerevisiae* can exist as a haploid, or can conjugate with a haploid of opposite mating type to form a diploid. Under low nutrient conditions, specifically a non-fermentable carbon source and nitrogen starvation (Freese et al., 1982), the diploid undergoes meiosis to form four daughter spores with a protective cell wall. Before the formation of the cell wall, the nascent spores must first be encapsulated in a double membrane referred to as the prospore membrane (PSM) (Neiman, 1998). The PSM initiates during Meiosis II at a protein plaque located on the spindle pole bodies, which are microtubule organizing centers similar to the centrosome in humans, and expands outward (Knop and Strasser, 2000). In *vps13*Δ the growth of the PSM is abnormal, and therefore, spores are not formed (Park and Neiman, 2012).

Although the full role of Vps13p in PSM formation has not been elucidated, recent evidence has pointed to Vps13p localizing to the PSM, and effecting PSM size and closure. During meiosis, Spo71p interacts with and promotes the localization of Vps13p to the PSM (Park et al., 2013). Spo71p itself localizes to the PSM during sporulation, and *spo71*Δ mutants display defects in PSM size and closure similar to *vps*13Δ mutants (Parodi et al., 2012; Park et al., 2013). *vps13*Δ mutants display decreased Phosphatidylinositol 4-phosphate in the PSM, which is the precursor of $PI(4,5)P_2$ (Park et al., 2013). The corresponding decrease in $PI(4,5)P_2$ is what is thought to be involved in the reduced PSM size (Park et al., 2013). $PI(4,5)P_2$ is an activator of a phospholipase D, Spo14p, which produces phosphatidic acid from phosphatidylcholine, and is essential for sporulation (Park et al., 2013). Overexpression of Spo14 rescues the reduced membrane size in *vps*13Δ mutants, but does not rescue the cytokinesis defect (Park et al., 2013). This indicates that the cytokinesis defect may be linked not to the reduced PA levels in the membrane, but to the reduced $PI(4,5)P_2$ levels (Park et al., 2013).

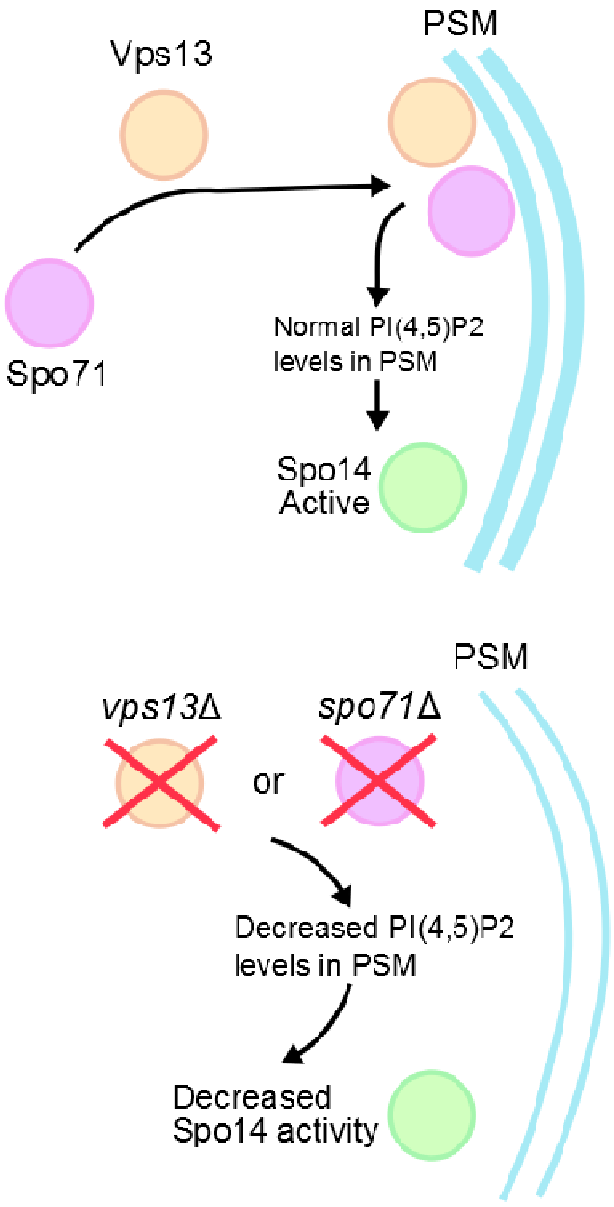

Figure 3 **The role of Vps13 in PSM size.**
Spo71 localizes Vps13 to the PSM during sporulation in *S. cerevisiae*. Vps13 promotes normal PI(4,5)P_2 levels in the PSM, which is an activator of Spo14. Deletion of *SPO71* or *VPS13*, results in decreased PI(4,5)P_2 pools in the PSM, which leads to reduced Spo14 activity and a smaller PSM.

1.2 **Mitochondrial homeostasis**

The final known role for Vps13p, in mitochondrial morphology and maintenance, was uncovered after a screen identified a synthetic lethality between *vps13*Δ and *mmm1*Δ in *S. cerevisiae* (Chan et al., 2006). Both *vps13*Δ and *mmm1*Δ mutants independently are viable, however in combination the deletions are lethal to the cell. Mmm1p is a transmembrane protein of the endoplasmic reticulum (ER), and is part of the ERMES complex that brings the ER and mitochondria to close proximity at junction points (Kornmann et al., 2009). Deletion of *MMM1* results in the mitochondria collapsing into large spherical organelles, which interferes with their segregation into daughter cells (Burgess et al., 1994). Mitochondria in *mmm1*Δ cells are also defective in respiration, and so the mutant cannot grow on a non-fermentable carbon source (Burgess et al., 1994). *mmm1*Δ mutants also have a defect in mitophagy, which is the process of removing damaged or unnecessary mitochondria from the cell (Böckler and Westermann, 2014). Interestingly, *vps13*Δ mutants show increased mitophagy, potentially indicating increased levels of mitochondrial damage (personal communication, Jae-Sook Park).

The ERMES complex was identified by a screen for mutants whose phenotype was suppressed by expression of an artificial tether between the ER and mitochondria (Kornmann et al., 2009). This screen uncovered Mmm1p, Mdm10p, Mdm34p, Mdm12p, as important components of the natural tether (Kornmann et al., 2009). Later Gem1p was discovered as an additional important regulatory component of the tether (Kornmann et al., 2011). Mmm1 is a transmembrane protein located in the endoplasmic reticulum (Kornmann et al., 2009). Mdm10 and Mdm34 are transmembrane proteins that span the outer mitochondrial membrane (Kornmann et al., 2009). Gem1 is a Miro GTPase of the outer mitochondrial membrane that has a proposed regulatory role for the ERMES complex, the specifics of which are not yet elucidated (Kornmann et al., 2011).

The phenotypes of *mmm1*Δ mutants are seen in deletions of the other components of the ERMES complex (Kornmann et al., 2009), so it is expected that

other members of the ERMES complex would be synthetically lethal with *vps13*Δ. High throughput screening has uncovered a synthetic lethality between *vps13*Δ and both *mdm12*Δ and *mdm10*Δ (Hoppins et al., 2011). Double deletion of *vps13*Δ and *mdm34*Δ leads to cell death, but *vps13*Δ and *gem1*Δ is not lethal (Personal communications, Jae-Sook Park). This suggests a potentially important interaction between Vps13p and the ERMES complex.

The close proximity of the ER and mitochondria created by the ERMES complex is important for many cellular processes. Disrupting the ERMES complex leads to a decreased exchange of phospholipids between the ER and mitochondria, suggesting the importance of the junction for phospholipid exchange (Kornmann et al., 2009). Several Ca^{2+} channels have been linked to the ER-mitochondrial junction point, and may play a role in controlling cytoplasmic Ca^{2+} levels (Rizzuto et al., 2004). Deletion of *MMM1*, *MDM12,* or *MDM10* leads to a defect of β-barrel protein assembly on the outer mitochondrial membrane (Wideman et al., 2010), and Mdm10p also has been found to localize with both the ERMES and SAM-holo complex (Yamano et al., 2010). Mitophagy is decreased in *mmm1*Δ, *mdm10*Δ, *mdm12*Δ, and *mdm34*Δ mutants, and autophagosomes localizes to sites near the ERMES complex, showing an important connection of the ERMES complex to mitophagy (Hamasaki et al., 2013). The junction site also serves as a localization point for peroxisomes and the pyruvate dehydrogenase complex, which converts pyruvate to acetyl-CoA for the citric acid cycle (Cohen et al., 2014). Thus, the ERMES complex and ER-mitochondrial junction points are linked to a variety of functions.

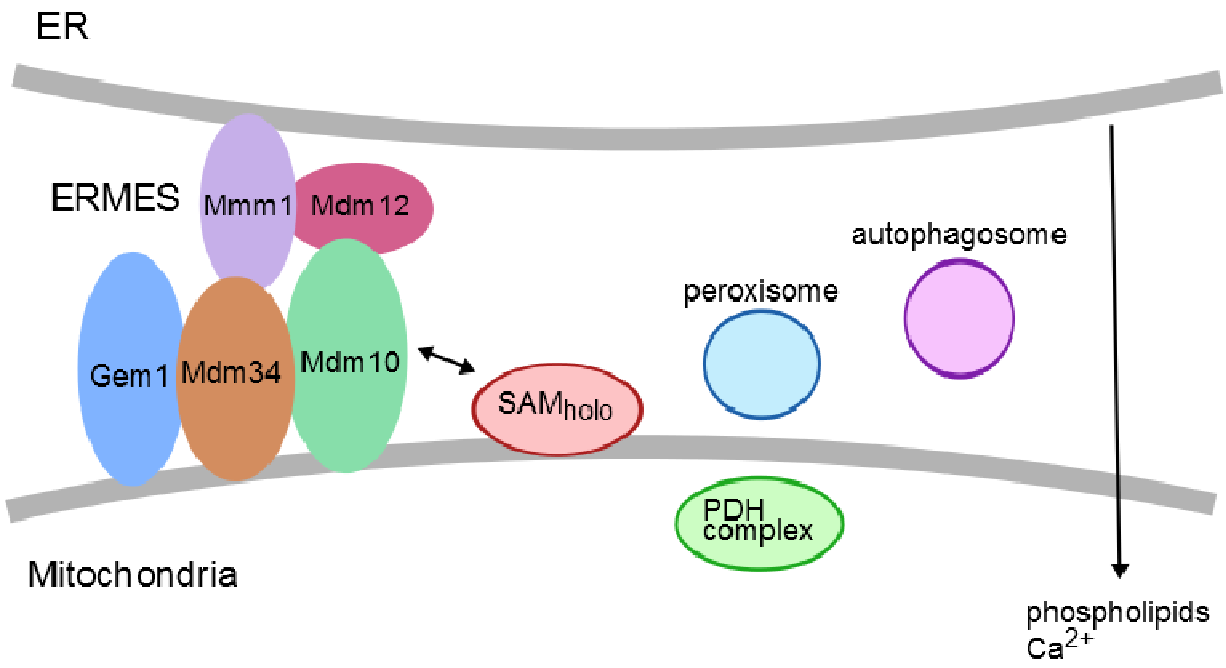

Figure 4 **The ERMES complex and the ER-mitochondrial junction.**
The ERMES complex consists of Mmm1, Mdm12, Mdm34, and Mdm10. Gem1 is a GTPase important for the regulation of the complex. Mdm10 is also a member of the SAM_{holo} complex which inserts β barrel proteins into the outer mitochondrial membrane. Peroxisomes and the PDH complex were found to localize to regions at the junction. The junction is an important region for transfer of certain phospholipids and Ca^{2+} to the mitochondria. Autophagosomes localize to the junction, and the junction is an important site for mitophagy.

1.3 **Summary of *VPS13***

Since its discovery in a screen for CPY sorting defects, Vps13 has emerged as an important protein with disparate roles in the cell. In addition, orthologs of *VPS13* are ubiquitous in many eukaryotic genomes (Rampoldi et al., 2001). Although the full structure and function has not yet been resolved, Vps13 has been implicated in three important roles in *S. cerevisiae*. First, Vps13p is important for endosome to TGN cycling of proteins, with *vps13*Δ mutants losing TGN transport of proteins such as Kex2p and Vps10p (Brickner and Fuller, 1997). Second, Vps13p is involved with PSM size and closure. Vps13p localizes to the PSM during sporulation via Spo71p, and *vps13*Δ mutants fail to form spores (Parodi et al., 2012; Park et al., 2013). These *vps13*Δ mutants do not complete cytokinesis, and have a decreased amount of $PI(4,5)P_2$, which decreases the function of Spo14, a phospholipase required for spore formation (Park and Neiman, 2012). Finally, a synthetic lethality exists between *vps13*Δ and *mmm1*Δ (Chan et al., 2006). The synthetic interaction between vps13 and ERMES complex mutants suggests that VPS13 may have an additional role in mitochondrial homeostasis.

2. ***VPS13A* and Chorea Acanthocytosis**

Uncovering the roles of *VPS13* in the yeast cell is of particular interest because of the connection of its ortholog, *VPS13A*, to the disease Chorea Acanthocytosis (ChAc) in humans (Dobson-Stone et al., 2002). ChAc is a rare, autosomal recessive, late onset neurodegenerative disease characterized by irregular hyperkinetic movement (chorea) and abnormally shaped, barbed, erythrocytes (acanthocytes) (Rampoldi et al., 2001). The neurodegenerative symptoms of ChAc are similar to the more common Huntington's disease, or Macleod's Syndrome (Dobson-Stone et al., 2002; Miki et al., 2010). *VPS13A* is one of four human orthologs of the yeast *VPS13* and has high conservation with *VPS13* found in *S. cerevisiae* (Rampoldi et al., 2001). The conservation between *VPS13* and *VPS13A* allowed for useful mapping of mutations from humans to yeast to further explore the role of *VPS13* in the cell and disease.

Most mutations in *VPS13A* isolated from ChAc patients lead to a *VPS13A* null mutant (Dobson-Stone et al., 2002). If the human protein is similarly multifunctional to the yeast protein, all of the activities the protein is involved in would be absent. This raises the question of which activity of Vps13A is relevant to the disease symptoms. There have been a handful of missense mutations identified that could possibly help to answer this question (Dobson-Stone et al., 2002; Tomiyasu et al., 2011; Rampoldi et al., 2001). These missense mutations might affect only one activity of Vps13A, and thus afford a unique opportunity to identify the function of *VPS13A* relevant to ChAc. By engineering the human missense alleles into *VPS13* in *S. cerevisiae*, it was possible to assay for CPY sorting, sporulation, and mitochondrial defects for these alleles.

The homology between the yeast *VPS13* and human *VPS13A* in both the size of the protein, and the four conserved regions, made finding target conserved amino acids affected by the missense mutations for the CRISPR/Cas engineering possible. Three missense alleles, *vps13-L66P*, *vps13-L1107P*, and *vps13-Y2702C,* were constructed in *VPS13* based on the human disease alleles *vps13A-L67P*, *vps13A-A1095P*, and *vps13A-Y2721C* respectively. After the *VPS13A* missense mutations with conserved residues in *VPS13* were engineered into *S. cerevisiae*, assays were performed for CPY sorting, sporulation, and mitochondrial defects. The CPY sorting assay was accomplished by western blot analysis of the CPY content both within and outside of the cell. The sporulation assay was performed by crossing haploids containing the missense mutations with a *vps13*Δ strain, sporulating the diploid, and then assessing for the presence of spores through microscopy. The mitochondrial defect assay was performed by engineering the missense mutations into a strain with chromosomal *MMM1* deleted, but containing a plasmid with wild-type *MMM1*. This strain was then plated on 5-FOA, which “kicks out” the plasmid, and the resulting *mmm1*Δ *vps13*Δ disease allele mutant was examined for growth. Two of these mutants, *vps13-L66P* and *vps13-Y2702C* were wild type for both the sporulation and CPY sorting functions, but displayed synthetic lethality in combination with *mmm1*Δ. This potentially suggests that the disease symptoms in ChAc patients is related to dysfunctions in mitochondrial homeostasis.

II. Methods

3. Strain Generation

3.1 RP201, RP202, and RP203

RP201, RP202, and RP203 (Table 2) were generated by first replacing thecods 66, 1107, and 2702 in *VPS13* with the kanamycin resistance gene (KanR) cassette in the BY4741 background strain (Table 2). These strains were then transformed with a CRISPR/Cas plasmid (generously donated by Gang Zhao) that targeted and cut the KanR gene, and a rescue oligonucleotide containing the appropriate missense mutation. Repair of the double strand break introduced by the Cas9 protein by homologous recombination with the repair oligonucleotide results in introduction of the missense mutation into the chromosome.

The KanR cassette from pFA6a-kanMX6 (Longtine et al., 1998) was first amplified by PCR using Phusion High-Fidelity DNA Polymerase (cat# M0530S, New England Biolabs), and the product was purified using the QIAquick PCR Purification Kit (cat# 28104, Qiagen). (i) Replacement of amino acid 66 with the KanR cassette required primers RCO3 and RCO4 (Table 1). (ii) Replacement of amino acid 1107 with the KanR cassette required primers RCO7 and RCO8 (Table 1). (iii) Replacement of amino acid 2702 with the KanR cassette required primers RCO12 and RCO13 (Table 1).

BY4741 was inoculated in 3 ml of YPD overnight at 30C. These cells were diluted into 50ml of YPD, incubated at 30C for 4 hours, and a LiAc transformation (Rose and Fink, 1990) was performed to transform the amplified KanR cassettes for integration through homologous recombination. Transformants were plated on G418 (Table 3) to select for successful integration of KanR cassette, and cells were grown for 3 days in 30C. KanR cassette insertion was confirmed by preparing genomic DNA using

a MasterPure Yeast DNA Purification Kit and (cat# MPY80200PCR, Epicenter) and PCR. (i) Replacement of codon 66 with the KanR cassette was confirmed with primers RCO9 and RCO17 (Table 1). (ii) Replacement of codon 1107 with the KanR cassette was confirmed with primers RCO14 and RCO66-R (Table 1). (iii) Replacement of codon 2702 with the KanR cassette was confirmed with primers RCO14 and JSO66R (Table 1).

In the second step these KanR cassette insertions were replaced with the correct missense mutation, using a CRISPR/Cas plasmid to form a double stranded break in the KanR gene. Using the LiAc procedure, 200 ng of this CRISPR/Cas plasmid was cotransformed with 1 nmol of rescue oligonucleotide to replace the KanR cassette with the missense mutation through homologous recombination. The following rescue oligonucleotides were used to generate the missense mutations. (i) *vps13-L66P* was generated using the rescue oligonucleotide RCO6 (Table 1). (ii) *vps13-L1107P* was generated using the rescue oligonucleotide RCO11 (Table 1). (iii) *vps13-Y2702C* was generated using the rescue oligonucleotide RCO15 (Table 1).

The transformants were plated on -Leu (Table 3) and grown for 3 days at 30C to select for successful transformation of the CRISPR/Cas plasmid. Loss of the KanR cassette was checked through replica plating onto G418, and correct insertion of the missense mutations was confirmed by sequencing of PCR fragments generated by amplification of the modified region.

3.2 **RP201S, RP202S, RP203S**

The diploid strains RP201S, RP202S, and RP203S were generated by crossing RP201, RP202, and RP203 to HI27, a *vps13*Δ strain (Table 2).

3.3 **RP301 and RP303**

RP303 was made as described for RP203 except for the following changes. Codon 2702 in *VPS13* was first replaced with the *SkHIS3* cassette in the LKM100

background strain (Table 2). This strain was then transformed with a CRISPR/Cas plasmid that targeted and cut the *SkHIS3* gene (generously provided by Sai Zhou), and a rescue oligonucleotide containing the appropriate missense mutation. The *SkHIS3* cassette from pFA6a-His3MX6 (Longtine et al., 1998) was amplified using the same primers as above. Finally, after the CRISPR/Cas transformation, loss of the *SkHIS3* cassette was checked through replica plating onto -His (Table 3).

In order to make RP301, it was necessary to first generate RP301K (Table 2). RP301K was made as described for RP201 except the AN117-16D background strain was used (Table 2). To generate RP301, RP301K was first crossed with JSP441 (Table 2). The resulting diploids were then sporulated on SPO media for 2 days, and dissected under microscopy to obtain haploids that grew on -Ura and G418.

4. CPY Sorting Assay

4.1 Preparation of cellular and growth media protein precipitates

RP201, RP202, RP203, BY4741, BY4741 *vps13*Δ, and BY4741 *vps10*Δ (Table 2) were inoculate in 3 ml of YPD and incubated overnight in a shaker at 30C. The cells were diluted with 2 ml of YPD and incubated for 4 hours in a shaker at 30C. The cells were then pelleted at 2,500 x g for 5 min, and the supernatant was carefully transferred into a clean tube.

4.2 Growth Media Protein Precipitate

A half volume of 100% TCA was added to the supernatant, and the sample was incubated on ice for 30 min. The sample was then centrifuged in a 4C centrifuge for 15 min at 16,000 x g, and the supernatant was discarded. 300ul of cold acetone was added, and the sample was centrifuged for 5 min at 16,000 x g in 4C centrifuge. The supernatant was disposed of and the pellet was air dried for 20 min at room temperature. The sample was then resuspended in 50ul of SDS sample buffer, and the pH was raised to pH5 using Tris-HCl pH7, indicated by change of the bromophenol blue

in the sample buffer from yellow to blue. The sample was then heated at 65C for 3 min, and centrifuged for 1 min at 16,000 x g before loading.

4.3 **Cellular Protein Precipitate**

The cell pellet was resuspended in 100ul of distilled H_2O, and 100ul of 0.2M NaOH was added to the sample. It was then incubated for 5 min at room temperature, centrifuged at 7,500 x g for 1 min, and then the supernatant was discarded. The pellet was resuspended in 50ul of SDS sample buffer, and the sample was heated at 65C for 3 min and centrifuged for 1 min at 16,000 x g before loading.

4.4 **Western blot analysis**

The samples were separated on an 8% polyacrylamide gel, and blotted to a PVDF transfer membrane. The membrane was blocked with 5% non-fat dry milk in TNET (10mM Tris-HCl, 2.5mM EDTA, 50mM NaCl, 0.05% Tween-20). The membrane was then probed with anti-CPY antibody (1:2000), and HRP linked anti-mouse secondary antibody. The membrane was visualize with ECL.

5. **Mitochondrial Assay - 5-FOA**

RP301, RP303, LKM100, and LKM100 with *vps13::SkHIS3* (Table 2) were plated onto 5-FOA containing plates as a screen for synthetic lethality of the double mutants, *vps13-L66P mmm1*Δ and *vps13-Y2070C mmm1*Δ respectively. RP301, RP303, LKM100, and LKM100 with *vps13::SkHIS3* were struck on 0.08% 5-FOA (Table 3) plates for single colonies. The cells were then grown for 3 days in a 30C incubator, and then the plates were visualized for the presence of individual colonies for each allele.

6. **Sporulation Assay**

RP201S, RP202S, RP203S, and RP200S (Table 2) were grown on YPD (Table 3) for 2 days 30C. These diploids were then replica plated to SPO (sporulation) media (Table 3) and incubated for 2 days at 30C. Slides were prepared by scraping a colony into 5µl of distilled H_2O placed on the slide, and viewed under a 40x objective with a

Zeiss Axioplan2 microscope (Carl Zeiss, Thornwood, NY). 200 cells per sample were counted and scored as either having spores or no spores.

oligo	sequence
RCO3	CATTAAATTTACCCATAGATGTGAAATCAGGGATACTGGGTGATTTGGTCCGGATCCCCGGGTTAATTAA
RCO4	TCGATAATGATTTCACGGGCTTATTCTTTAAACTTGACCATGGGACGGTGAATTCGAGCTCGTTTAAAC
RCO5	CCTTCCTCATCTTCAACC
JSO78	GTGACTACCAAAAGGGAAAA
RCO6	AATTTACCCATAGATGTGAAATCAGGGATACTGGGTGATTTGGTCCCCACGGTCCCATGGTCAAGTTTAAAGAATAAGCCC GTGAAAATCATT
RCO7	CGGCTGGTGAATTCACAATGGTTTTACTACCGGAAAGATACAACATTAACCGGATCCCCGGGTTAATTAA
RCO8	CTGGAAAACGATTCATTTGTTTCATCAGTCAACTCCAACCCGCCTAATTTGAATTCGAGCTCGTTTAAAC
RCO9	TACGGATCCTAACGCTCC
RCO17	CATGCATAGAGCCCGTAG
RCO11	TCACAATGGTTTTACTACCGGAAAGATACAACATTAACCCAAAATTAGGCGGGTTGGAGTTGACTGATGAAACAAATGA
RCO12	TTACGRTATTAATCCAGGAATTTTCCATACAATTAGATGAAGACATGCTGCGGATCCCCGGGTTAATTAA
RCO13	GAATCCATGATCCATGGGGATCCTGGGAATTTTATGAAGTCCATCATAGCGAATTCGAGCTCGTTTAAAC
RCO14	ACGGTGGGCTGAATATGG
JSO66-R	GATGAGGATGAGAAGGTTAATACAC
RCO15	TCCAGGAATTTTCCATACAATTAGATGAAGACATGCTGTGTGCTATGATGGACTTCATAAAATTCCCAGGATCCCCATG

Table 1 **Oligonucleotides used in this study.**

strain	genotype	notes
BY4741	*MATa his3* leu*2 ura3 met15*	
RP201	*MATa his3 leu2 ura3 met15 vps13-L66P*	*vps13-L66P* in BY4741 background
RP202	*MATa his3 leu2 ura3 met15 vps13-L1107P*	*vps13-L1107P* in BY4741 background
RP203	*MATa his3 leu2 ura3 met15 vps13-Y2702C*	*vps13-Y2702C* in BY4741 background
KO collection	*MATa his3 leu2 ura3 met15 mmm1*::*KanR*	BY4741 background
LKM100	*MATa his3 leu2 ura3 met15 mmm1*::*KanR*, plus pRS316-*MMM1*	plasmid added to KO collection
RP301	*MATa his3 leu ura trp mmm1*::*KanR vps13-L66P*, plus pRS316-*MMM1*	*vps13-L66P* in LKM100
RP303	*MATa his3 leu2 ura3 met15 mmm1*::*KanR vps13-Y2702C*, plus pRS316-*MMM1*	*vps13-Y2702C* in LKM100
HI27	*MATα vps13*Δ::*his5+ ura3 his3*Δ*SK trp1*::*hisG arg4-NspI lys2 ho*Δ::*LYS2 rme1*Δ::*LEU2 leu2*	SK1 background
RP201S	*MATa/MATα ura3/ura3 leu2/leu2 met15 his3 his3*Δ*SK trp1*::*hisG arg4-NspI lys2 ho*Δ::*LYS2 rme1*Δ::*LEU2 vps13*Δ::*his5+/vps13-L66P*	RP201 crossed with HI27
RP202S	*MATa/MATα ura3/ura3 leu2/leu2 met15 his3 his3*Δ*SK trp1*::*hisG arg4-NspI lys2 ho*Δ::*LYS2 rme1*Δ::*LEU2 vps13*Δ::*his5+/vps13-L1107P*	RP202 crossed with HI27
RP203S	*MATa/MATα ura3/ura3 leu2/leu2 met15 his3 his3*Δ*SK trp1*::*hisG arg4-NspI lys2 ho*Δ::*LYS2 rme1*Δ::*LEU2 vps13*Δ::*his5+/vps13-Y2702C*	RP203 crossed with HI27
RP200S	*MATa/MATα ura3/ura3 leu2/leu2 met15 his3 his3*Δ*SK trp1*::*hisG arg4-NspI lys2 ho*Δ::*LYS2 rme1*Δ::*LEU2 vps13*Δ::*his5+/vps13*::*SkHIS3*	
AN117-16D	*MATa his3 ura3 trp1-hisG leu2 lys2 hoD::LYS2*	
RP301K	*MATa his3 ura3 trp1-hisG leu2 lys2 hoD::LYS2 vps13-L66P*	SK1 background
JSP441	*MATα his3 leu trp ura mmm1::KanR, plus* pRS316-*MMM1*	

Table 2 **Strains used in this study.**

plate	contents	notes
YPD	2% agar, 2% bactopeptone, 1% yeast extract, 2% dextrose	complete media
SPO	2% difco agar, 1% potassium acetate, 0.05% yeast extract, 0.05% dextrose, 0.05% -arg dropout media	sporulation assay
5-FOA	2% agar, 0.7% yeast nitrogen base w/o a.a, 2% dextrose, 0.2% dropout, 0.08% 5-FOA	mitochondrial assay
SD dropout	2% agar, 0.7g yeast N base w/o a.a., 2%dextrose, 0.2% dropout powder	selectable markers
LB+Amp	2% agar, 1% tryptone, 0.5% NaCl, 0.5% yeast extract, 0.1 mg/ml AMP	E. coli with plasmid
G418	2% agar, 1% tryptone, 0.5% NaCl, 0.5% yeast extract, 20 mg/ml G418	checking KanR cassette

Table 3 **Media used in this study**.

III. Results

7. Alignments of *VPS13* and *VPS13A* identify cognate residues of disease mutations.

Cognate residues for three missense mutations found in *VPS13A* of ChAc patients were identified in *VPS13* of *S. cerevisiae* after analysis of Blastp sequence alignment. (i) A Leu to Pro mutation of amino acid 67 in *VPS13A* (Tomiyasu et al., 2011) was aligned to a Leu on amino acid 66 in *VPS13* of *S. cerevisiae* (Figure 5). This residue falls within the N-chorein domain (Figure 7) which is conserved to *VPS13A* (Hayashi et al., 2012, Velayos-Baeza et al., 2004). (ii) An Ala to Pro mutation of amino acid 1095 in *VPS13A* (Dobson-Stone et al., 2002) was aligned to a Leu on amino acid 1107 in *VPS13* of *S. cerevisiae* (Figure 5). This residue resides within the region between the N-chorein and DUF domain (Figure 7) that is conserved to *VPS13A* (Velayos-Baeza et al., 2004). (iii) A Tyr to Cys mutation of amino acid 2721 in *VPS13A* (Rampoldi et al., 2001) was aligned to a Tyr on amino acid 2702 in *VPS13* of *S. cerevisiae* (Figure 5). This residue is in the region of conservation on the C terminal domain (Figure 7) that is conserved to *VPS13A* (Hayashi et al., 2012, Velayos-Baeza et al., 2004). Because these three residues were clearly orthologous, And the conserved regions they fall within in Vps13 are conserved to Vps13A (Hayashi et al., 2012, Velayos-Baeza et al., 2004), they were chosen for introduction of the mutations into the yeast gene.

VPS13A residue	Sequence Alignment
67	Vps13: 61 LGDLVLTVPWSSLKNKPVKIIIEDCYLLCSPRS 93 +G+L L +PW +L +PV+ ++E+ YLL P S Vps13A: 62 IGNLKLIIPWKNLYTQPVEAVLEEIYLLIVPSS 94
1095	Vps13: 1089 LSAGEFTMVLLPERYNINLKLGGLELTDETNESFSRDSVFRKIIQMKGQELVELSYESFD 1148 + + M++ P IN KL + + D ++++K + + G+E+ S+ Vps13A: 1077 IEGLDSEMIMRPSETEINAKLRNIIVLDS-----DITAIYKKAVYITGKEVFSFKMVSYM 1131
2721	Vps13: 2670 SKVNDSLQAVPYFKHVTLLIQEFSIQLDEDMLYAMMDFIKFPGSPWIMDSRDYKYDEEIQ 2729 + + K+ +LIQE ++LD +YA+ D +M + + E++ Vps13A: 2689 VMRSAGHSQISRIKYFKVLIQEMDLRLDLGFIYALTD---------LMTEAEVTENTEVE 2739

Figure 5 **Sequence alignment between *VPS13* and *VPS13A* in the mutated regions.** The residue of the *VPS13A* missense mutations found in the sequencing of ChAc patients, amino acids 67, 1095, and 2721, were aligned with *VPS13* in *S. cerevisiae* using Blastp to look for conserved cognate residues.

8. **Engineering of missense mutations into *VPS13* of S. cerevisiae.**

A CRISPR/Cas strategy (DiCarlo et al., 2013) was used to introduce the missense mutations, *vps13-L66P, vps13-L1107P, and vps13-Y2702C* (Figure 7) into the endogenous *VPS13* locus. To generate the strains for assay of sporulation and CPY sorting, the codon to be mutated was first replaced by integration of KanR cassette using PCR-mediated homologous integration (Longtine et al., 1998) in the strain BY4741. Next, the resulting strains were co-transformed with a plasmid expressing the endonuclease Cas9 and a guide RNA designed to target the KanR gene as well as a single stranded oligonucleotide containing the desired nucleotide containing 40 nt both 5' and 3' of the desired point mutations. Expression of the Cas9 and guide RNA leads to a double strand break within the KanR gene. This break can be healed by homologous recombination between the broken chromosome and the oligonucleotide resulting in removal of KanR and introduction of the mutation coded in the oligonucleotide. Co-transformants with the CRISPR/Cas9 plasmid and rescue oligonucleotides were selected on –Leu media (which selects for the CRISPR/Cas plasmid) and then subsequently screened by replica plating to identify transformants that had lost the KanR marker. The mutagenized region was then amplified by PCR from these candidates and sequenced to confirm the introduction of the desired point mutation. Strains for analysis of the mitochondrial phenotype were generated by the same strategy except that the codons were first replaced by a cassette with the *S. kluyveri HIS3* gene (and subsequently transformed with a Cas9 plasmid expressing a *SkHIS3* directed guide RNA) and that the mutations were introduced into an *mmm1*Δ strain carrying the wild-type *MMM1* on a *URA3* plasmid.

All three alleles were successfully introduced into BY4741, while the *vps13-L66P* and *vps13-Y2702C* alleles were also successfully introduced into LKM100 (Figure 6). *vps13-L1107P* was not generated in the LKM100 background because successful transformants could not be obtained. The five strains that were successfully obtained were then used for further analyses.

strain	alignment
RP201	Query: 232 AACTTGACCATGGGACCGTGGGGACCAAATCACCCAGTATCCCTGATTTCACATCTATGG 173 VPS13 63429 AACTTGACCATGGGACCGTTAAGACCAAATCACCCAGTATCCCTGATTTCACATCTATGG 63488
RP202	Query: 168 AACCCGCCTAATTTTGGGTTAATGTTGTATCTTTCCGGTAGTAAAACCATTGTGAATTCA 109 VPS13: 60311 AACCCGCCTAATTTTAAGTTAATGTTGTATCTTTCCGGTAGTAAAACCATTGTGAATTCA 60370
RP203	Query: 374 TTATGAAGTCCATCATAGCACACAGCATGTCTTCATCTAATTGTATGGAAAATTCCTGGA 315 VPS13: 55521 TTATGAAGTCCATCATAGCATACAGCATGTCTTCATCTAATTGTATGGAAAATTCCTGGA 55580
RP301	Query: 240 ACTTGACCATGGGACCGTGGGGACCAAATCACCCAGTATCCCTGATTTCACATCTATGGG 181 VPS13: 63430 ACTTGACCATGGGACCGTTAAGACCAAATCACCCAGTATCCCTGATTTCACATCTATGGG 63489
RP303	Query: 344 TTTATGAAGTCCATCATAGCACACAGCATGTCTTCATCTAATTGTATGGAAAATTCCTGG 285 VPS13: 55520 TTTATGAAGTCCATCATAGCATACAGCATGTCTTCATCTAATTGTATGGAAAATTCCTGG 55579

Figure 6 **Sequencing results of missense mutation strains**.
The CRISPR/Cas genetic engineering system was used to insert the missense mutations *vps13-L66P*, *vps13-L1107P*, and *vps13-Y2702C* into the BY4741 and LKM100 strains of *S. cerevisiae*. *vps13-L1107P* was not generated in the LKM100 strain. Sequencing of the PCR fragment of the region containing the mutation was aligned to *VPS13* using Blastn analysis to check for correct integration of the mutations. The query sequence represents the PCR fragment that was sequenced.

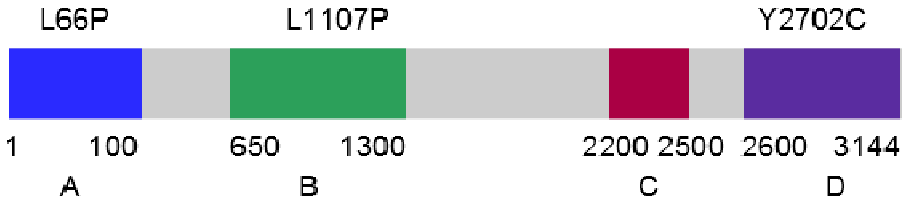

Figure 7 ***VPS13* missense mutation locations in *S. cerevisiae***.
Three missense mutations were engineered into *VPS13* of *S. cerevisiae*. *vps13-L66P* is located in the N-chorein domain (A). *vps13-L1107P* is in the conserved region (C) between amino acids 650 and 1300. vps13-Y2702C sits within the conserved C terminus (D). No missense mutants were engineered into the DUF1162 domain (C).

9. **All three human alleles support sporulation in yeast.**

To check for the effects of the *vps13-L66P, vps13-L1107P, and vps13-Y2702C* missense mutations on sporulation efficiency, RP201, RP202, and RP203 were first crossed to a *vps13*Δ deletion strain, HI27, to generate diploid strains that are hemizygous for the disease allele. These diploids were then sporulated on SPO media, and the percentage of cells with spores present was counted by microscopy (Figure 8).

All three diploids carrying the human alleles displayed a sporulation efficiency comparable to the wild-type control, and vastly greater than a *vps13*Δ strain. Thus, the *vps13-L66P, vps13-L1107P,* and *vps13-Y2702C* mutations do not interfere with the ability of the yeast protein to promote sporulation.

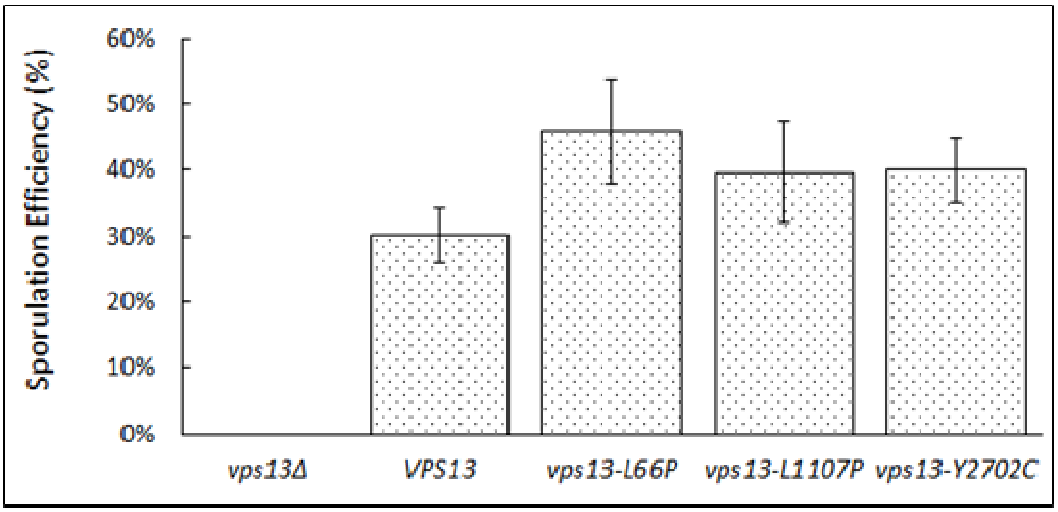

Figure 8 **Sporulation efficiency of mutant strains.**
The *VPS13*, *vps13*Δ, *vps13-L66P*, *vps13-L1107P*, and *vps13-Y2702C* strains in the BY4741 background were crossed to HI27, and then sporulated for 2 days. HI27 is a *vps13*Δ mutant in the SK1 background. The ratio of cells with and without spores in the ascus was counted using microscopy. A total of 1000 cells were counted for the missense mutants, and 600 were counted for *VPS13* and *vps13*Δ. The error bars represent standard deviation.

10. *vps13-L66P* and *vps13-Y2702C* support normal CPY sorting

To examine the ability of the human alleles to support normal TGN-endosome traffic, the delivery of CPY to the vacuole was assessed by Western blot analysis in all three mutant strains as well as *VPS13*, *vps10*Δ and *vps13*Δ control strains. Cells were grown to saturation in liquid medium, and the medium was cleared of cells by centrifugation. Total cellular protein was extracted from the cell pellet (Rose and Fink, 1990) and the protein in the growth media of the cells was concentrated by a TCA protein precipitation. The resulting protein samples were then examined by Western blot using anti-CPY antibodies (Figure 9).

In the wild-type control, a strong band corresponding to the mature, vacuolar-localized CPY was seen in the pellet. While some mature protein was also seen in the supernatant fraction (presumably from intact cells that did not pellet in the centrifugation) no higher molecular weight forms indicative of missorting were seen (Figure 9). In both the *vps10*Δ and *vps13*Δ control strains known to secrete CPY, the higher molecular weight immature form of the protein can be seen in the supernatant fraction (Figure 9).

In the mutant strains carrying the *vps13-L66P* and *vps13-Y2702* alleles, only the band for the 61 kDa mature form of CPY is seen, comparable to the wild type *VPS13* strain (Figure 9). Thus, there was no detectable secretion of CPY from the *vps13-L66P* and *vps13-Y2702C* strains. By contrast, in the supernatant fraction from the *vps13-L1107P* strain the higher molecular weight form of CPY was visible. While the fraction of CPY secreted by *vps13-L1107P* appears somewhat lower than in *vps13*Δ, these results indicate that this allele affects the CPY sorting function of *VPS13*. Interestingly, however, the *vps13-L66P* and *vps13-Y2702C* alleles are apparently wild-type for this function.

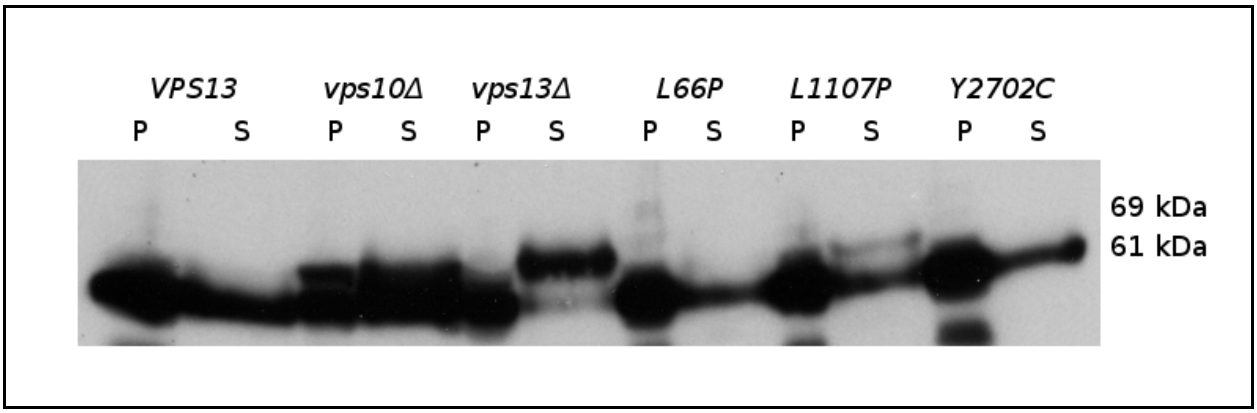

Figure 9 **Western blot analysis of CPY secretion from *VPS13* mutants**.
The *VPS13*, *vps10*Δ, *vps13*Δ, *vps13-L66P*, *vps13-L1107P*, and *vps13-Y2702C* strains in the BY4741 background were assayed for the 61 kDa mature form of CPY, and the 69 kDa precursor form of CPY in the cellular and growth media protein precipitates. “S” represents the growth media protein precipitate, and “P” represents the cellular protein precipitate. The cellular precipitate was diluted by 1:10 before loading.

11. ***vps13-L66P* and *vps13-Y2702C* are synthetically lethal with *mmm1*Δ**

The possible interaction of *vps13-L66P*, or *vps13-Y2702C* with an ERMES mutation were tested in the strains RP301 and RP303 which carry the two disease alleles, respectively, along with an *mmm1*Δ covered with the *MMM1* on a *URA3* based plasmid. *vps13-L1107P* was not tested because we were unable to generate the proper strain. In order to examine the potential synthetic lethality between the missense mutants and *mmm1*Δ, the strains were grown without selection for the *URA3*, and then transferred to plates containing the drug 5-fluoroorotic acid (5-FOA).

5-FOA is taken up by wild-type yeast and converted to the toxic product 5-fluoro-uracil (Boeke et al., 1987). However mutation of the uracil biosynthetic gene *URA3* blocks the conversion and thus allows growth in the presence of the drug. Thus, only if the *URA3 MMM1* plasmid is lost from strains RP301 and RP303 can the cells grow on 5-FOA. However, loss of the plasmid also reveals the *mmm1*Δ phenotype, so the cells that have lost the plasmid can only grow if the *VPS13* allele present can provide the mitochondrial function of *VPS13*. For example, the *vps13*Δ *mmm1*Δ strain with the *MMM1* containing plasmid grows on both YPD and -Ura media, however, there is no growth of that strain on the 5-FOA plate (Figure 10). This is in contrast to the strain that has *VPS13 mmm1*Δ, which is not lethal because *mmm1*Δ alone is not lethal. When the *MMM1* containing plasmid is lost after being plated on 5-FOA, the strain still grows (Figure 10). When RP301 and RP303 are plated onto 5-FOA, cells did not grow on 5-FOA after successfully growing on both -Ura and YPD (Figure 10). This is similar to *vps13*Δ *mmm1*Δ, and indicates that *vps13-L66P* and *vps13-Y2702C* have a lethal defect in combination with *mmm1*Δ. Thus, these two alleles appear to be uniquely defective in the mitochondrial homeostasis function of *VPS13*.

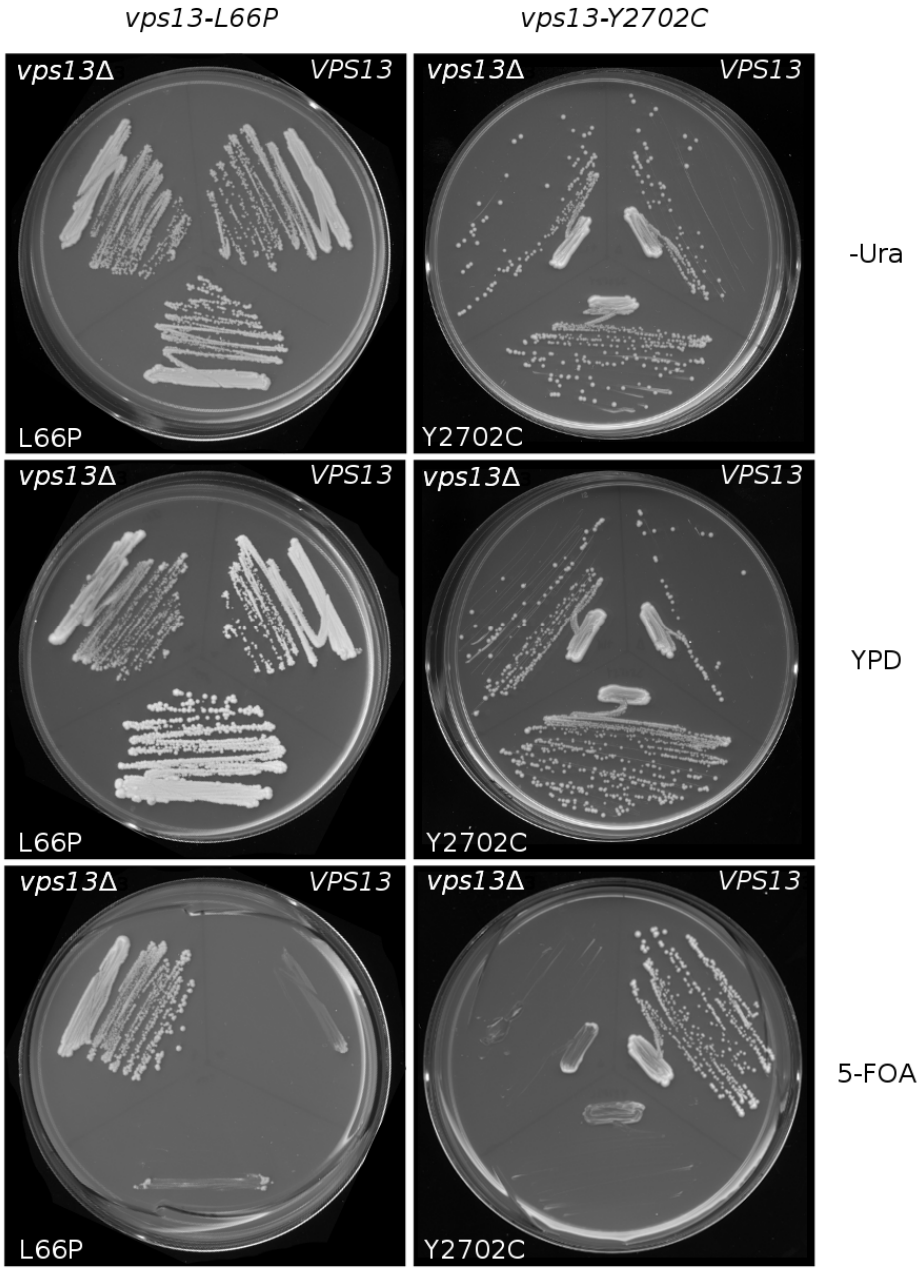

Figure 10 **Viability of *VPS13* mutants with *mmm1*Δ**.
*vps13*Δ, *vps13-L66P*, and *vps13-Y2702C* mutations were generated in the LKM100 strain, and plated onto YPD, -Ura, and 5-FOA for 3 days and the presence of growth was checked. LM100 was generated by transforming the plasmid pRS316-*MMM1* into the *mmm1*Δ KO collection. The top left colonies on the plates are LKM100, the top right colonies are LKM100 with *vps13*::*HIS3*, and the bottom colonies on the plates are *vps13-L66P* and *vps13-Y2702C* in LKM100.

IV. Discussion

Vps13 is a large conserved protein with seemingly disparate roles in *S. cerevisiae*. These include vesicular traffic between the endosome and TGN (Bankaitis et al., 1986), a connection to mitochondrial maintenance and morphology (Chan et al., 2006), and a role in PSM size and closure (Park and Neiman, 2012). Mutations in the human *VPS13* ortholog, *VPS13A*, have been uncovered in patients with a rare autosomal recessive disease, chorea acanthocytosis (Dobson-Stone et al., 2002). Three human missense mutations in *VPS13A* were aligned to cognate residues in *VPS13*, and these missense mutations were then engineered into *S. cerevisiae*. Assays were then run to check for mitochondrial, sporulation, and CPY sorting defects to look for separation of function mutants to better understand its role in the cell, and to look for clues on the role of *VPS13A* in chorea acanthocytosis. It was found that the missense mutations *vps13-L66P* and *vps13-Y2702C* were synthetically lethal in combination with an *mmm1*Δ mutant, and that *vps13-L1107P* missorted CPY out of the cell (Table 4). Furthermore, none of the missense mutants were defective in sporulation (Table 4).

	CPY Missorting	Spore Formation Defect	Lethality with *mmm1*Δ
vps13-L66P	no	no	yes
vps13-L1107P	yes	no	not obtained
vps13-Y2702C	no	no	yes

Table 4 **Summary of assay results.**
vps13-L1107P is defective in CPY transport, and missorted CPY out of the cell upon western blot analysis. None of the mutants had sporulation efficiencies affected when crossed to HI27 and sporulated. Both *vps13-L66P* and *vps13-Y202C* were synthetically lethal in combination with *mmm1*Δ.

vps13-L1107P results in the missorting of CPY from *S. cerevisiae*, whereas *vps13-L66P and vps13-Y2702C* do not. Vps13 is required for the recycling of the CPY sorting receptor Vps10 back to the TGN from the late endosome (Marcusson et al., 1994). *vps13*Δ mutations result in the loss of TGN localization of Vps10, which then results in CPY missorting (Marcusson et al., 1994). It is possible that the missense mutation *vps13-L1107P* results in the loss of the ability for Vps13 to properly recycle Vps10 back to the TGN. Amino acid 1107 in Vps13 sits within the conserved region sitting between the N-chorein domain and DUF1162 (Figure 7). It is possible that this region plays a role in Vps13's ability to properly recycle proteins back to the TGN through a yet unknown interaction. It is interesting to note that the other missense mutations, *vps13-L66P and vps13-Y2702C*, sit on the conserved N and C terminus respectively (Figure 7), and sort CPY normally. Whether these conserved domains or targeted regions are important for proper recycling of Vps10 back to the TGN would also require further study.

The CPY missorting in the *vps13-L1107P* mutant may be indicative of a more widespread vesicular trafficking defect between the late endosome and TGN. *VPS13* deletion mutants have also been found to lose TGN localization of the protease Kex2p (Brickner and Fuller, 1997), and the aminopeptidase DPAP-A (Bowers and Stevens, 2005), suggesting a role for *VPS13* beyond just Vps10. The loss of TGN localization of Kex2p, DPAP-A, and Vps10 is not unique to *vps13*Δ mutants, sharing a similar phenotype with mutants defective in the retromer complex (Pfeffer, 2001). The retromer complex is a highly conserved complex with homologs found in both *S. cerevisiae* and mammals that is important in the recycling of proteins from the late endosome to TGN (Bonifacino and Hurley, 2008). Interestingly, a component of the retromer in humans, Vps35p, has been implicated in late onset Parkinson's Disease, a neurodegenerative disease (Zimprich et al., 2011). It is important to note that both the *vps13-L66P and vps13-Y2702C* missense mutations did not missort CPY, which indicates that if *VPS13A* does have a role in endosome to TGN trafficking, it may not be the primary basis for the disease symptoms of ChAc.

All of the missense mutants, *vps13-L66P, vps13-L1107P, and vps13-Y2702C,* produced spores at a percentage similar to wild type *VPS13* in *S. cerevisiae*. Vps13 both localizes to and affects the size and closure of the PSM during sporulation. *vps13*Δ mutants have reduced $PI(4,5)P_2$ levels in the PSM during sporulation, effecting the function of Spo14, and these mutants also cannot complete cytokinesis of the PSM (Park and Neiman, 2012). *vps13-L66P, vps13-Y2702C, and vps13-L1107P* sit within the conserved N and C terminus, as well as the conserved region between the N-chorein and DUF1162 domain respectively (Figure 7). The lack of sporulation defect in these mutants could indicate that these domains, or the targeted regions within them, are not important for the role that Vps13 has in sporulation. However, the connection between the analogous missense mutations in *VPS13A* and chorea acanthocytosis is still not yet clear.

Vps13A plays a role in the morphology of red blood cells as evidenced by the acanthocytes seen in patients with chorea acanthocytosis (Tomiyasu et al., 2011). Epb41 is a protein that helps to link the spectrin and actin cytoskeleton of erythrocytes with the plasma membrane (Salomao et al., 2008). Mutations in Epb41 have been linked to elliptocytosis, in which a majority of red blood cells have an abnormal shape (Gallagher, 2004). $PI(4,5)P_2$ binding is important for the regulation of the interaction between Epb41 and plasma membrane proteins (An et al., 2006). *vps13*Δ mutants in *S. cerevisiae* have decreased $PI(4,5)P_2$ in the PSM during sporulation, so it is possible that Vps13A affects the levels of $PI(4,5)P_2$ in the plasma membrane of erythrocytes (Park and Neiman, 2012). Although the missense mutations in this study do not provide further evidence of this interaction, it is still of interest to uncover the how or if Vps13 directly influences membrane $PI(4,5)P_2$ levels.

When the *S. cerevisiae* LKM100 strain was engineered with the missense mutations *vps13-L66P* and *vps13-Y2702C*, the cells were no longer viable. Independently, *vps13*Δ and *mmm1*Δ deletions are viable, however, in combination they are lethal (Chan et al., 2006). Amino acid 66 of Vps13 sits within the N-chorein domain, and amino acid 2702 sits within the conserved C terminal domain, so It is possible that

both of these domains are important for a yet unknown function that is tied to mitochondrial maintenance and morphology, however, more study of these domains would be necessary (Figure 7). The connection between Vps13 and Mmm1 has yet to be elucidated, but the abrogation of cell viability could be tied to Mmm1's role in the ERMES complex. The ERMES complex brings the ER and mitochondria to close proximity at contact sites, and both the complex and physical proximity of the structures are important for functions such as the insertion of β-barrel proteins into the outer mitochondrial membrane, lipid and Ca^{2+} transport, and mitochondrial maintenance and morphology (Kornmann, 2013). Disruption of any component of the ERMES complex results in phenotypes similar to that of an *mmm1*Δ mutant (Kornmann et al., 2009), and all members in the ERMES complex except *GEM1* are synthetically lethal with vps13Δ(Hoppins et al., 2011, Personal communications, Jae-Sook Park). Thus, it is probable that the synthetic lethality with *mmm1*Δ is indicative of a larger problem of the ERMES complex.

When the ERMES complex is disrupted, there is a compensatory response from the vacuole in which contacts between the vacuole and mitochondria are expanded at mitochondrial contact sites which are created by the protein complex vCLAMP (Elbaz-Alon et al., 2014). The vCLAMP consists of Vps39 and Ypt7, and serves to bring the vacuole and mitochondria into close proximity (Klecker and Westermann, 2014). Inversely, in *vps39*Δ mutants, when the vCLAMP is disrupted, contacts between the ER and mitochondria are expanded (Elbaz-Alon et al., 2014). These contact sites serve as important transport sites of phospholipids, and when both the ERMES and vCLAMP are deleted, phospholipid transport is disrupted, which is lethal to the cell (Elbaz-Alon et al., 2014). One possible explanation for the synthetic lethality of *vps13*Δ and *mmm1*Δ is that VPS13 plays some role in the function of vCLAMP. It is possible that disrupting *VPS13* affects the ability for the vacuole to exchange phospholipids with the mitochondria, which would result in cell death when *MMM1* is also deleted. *vps13*Δ mutants have reduced $PI(4,5)P_2$ levels in the PSM (Park and Neiman, 2012), so it is possible that the pool of available $PI(4,5)P_2$ for transport across the vacuolar-mitochondrial contact site is reduced.

Though the ERMES complex proteins have no direct orthologs in human cells, mitochondrial contact sites with similar functions to ERMES do exist (Kornmann, 2013). Recently, it has been uncovered that autophagosomes originate near the ER-mitochondrial contact sites of mammals (Hamasaki et al., 2013). Double membrane bound autophagosomes are responsible for engulfing and delivering intracellular contents bound for lysosomal degradation or recycling in a process important for cell homeostasis (Hamasaki et al., 2013). Disruption of the ER-mitochondrial contact sites results in the loss of autophagosome formation (Hamasaki et al., 2013). In mice deficient for autophagy in neural cells, there was neurodegeneration in response to the aggregation of abnormal proteins in the cytoplasm (Hara et al., 2006). *vps13*Δ mutants in *S. cerevisiae* actually have increased mitophagy, a form of autophagy for damaged or unneeded mitochondria (personal communications, Jae-Sook Park and Aaron Neiman). It is possible that this increased mitophagy interferes with the generation of autophagosomes at the ER-mitochondrial contact sites. Although *vps13-L66P* and *vps13-Y2702C* were not directly assayed for autophagy defects, or increased mitophagy, it is possible that this defect exists in *S. cerevisiae* in those mutants, and is connected to an autophagy defect in humans.

Although *vps13-L1107P* was not successfully engineered into the LKM100 strain, it is expected that *vps13-L1107P* would also be synthetically lethal with *mmm1*Δ because of the synthetic lethality of the other mutants. If this strain is generated and it is synthetically lethal, then it would further support ChAc being a disease related to mitochondrial maintenance. This would be true despite there being a CPY sorting defect of *vps13-L1107P*, because the other mutants did not have this defect. The fact that the other mutants did not have a CPY sorting defect would also support the idea that even if *vps13-L1107P* was not synthetically lethal with *mmm1*Δ, that is does not necessarily mean that ChAc is a disease of protein retention in the TGN. Despite the outcome, generation of this strain and testing for synthetic lethality is important for helping to elucidate the role of *VPS13* in the cell.

Missense mutations in *VPS13A* were uncovered after the sequencing of this gene in patients with ChAc. These missense mutations were engineered into the cognate residues of the *VPS13A* homolog in *S. cerevisiae*, *VPS13*, in the strains LKM100, and BY4741 to perform assays for CPY sorting defects, sporulation efficiency, and synthetic lethality with *mmm1*Δ. The results of these assays provided clues to the role of Vps13A in the cell and disease. It is proposed that the primary neurodegenerative symptoms of ChAc are caused by aberrant maintenance and phospholipid transport at the mitochondria. Further studies would focus on phospholipid exchange and mitophagy in both the yeast and mammalian model, which could help uncover the role of *VPS13* and its ortholog in humans. Interestingly, mutations in *VPS13B*, one of the other four orthologs of *VPS13*, has been found to cause a developmental disease, Cohen Syndrome (Balikova et al., 2009). Although missense mutants were found in the sequencing of Cohen Syndrome patients, there were no apparent cognate residues in *VPS13* found after Blastp alignment, so this disease was not considered in the study. However, it would be interesting to further study this disease. Nevertheless, uncovering the role of *VPS13A* in ChAc patients could possibly lead to clues for therapeutic treatments of the disease.

Bibliography

An, X., Zhang, X., Debnath, G., Baines, A.J., and Mohandas, N. (2006). Phosphatidylinositol-4,5-Biphosphate (PIP_2) Differentially Regulates the Interaction of Human Erythrocyte Protein 4.1 (4.1R) with Membrane Proteins †. Biochemistry *45*, 5725–5732.

Balikova, I., Lehesjoki, A.-E., de Ravel, T. j. l., Thienpont, B., Chandler, K. e., Clayton-Smith, J., Träskelin, A.-L., Fryns, J.-P., and Vermeesch, J. r. (2009). Deletions in the VPS13B (COH1) gene as a cause of Cohen syndrome. Hum. Mutat. *30*, E845–E854.

Bankaitis, V.A., Johnson, L.M., and Emr, S.D. (1986). Isolation of yeast mutants defective in protein targeting to the vacuole. PNAS *83*, 9075–9079.

Böckler, S., and Westermann, B. (2014). Mitochondrial ER Contacts Are Crucial for Mitophagy in Yeast. Developmental Cell *28*, 450–458.

Boeke, J.D., Trueheart, J., Natsoulis, G., and Fink, G.R. (1987). 5-Fluoroorotic acid as a selective agent in yeast molecular genetics. Meth. Enzymol. *154*, 164–175.

Bonifacino, J.S., and Hurley, J.H. (2008). Retromer. Curr Opin Cell Biol *20*, 427–436.

Bowers, K., and Stevens, T.H. (2005). Protein transport from the late Golgi to the vacuole in the yeast Saccharomyces cerevisiae. Biochimica et Biophysica Acta (BBA) - Molecular Cell Research *1744*, 438–454.

Brickner, J.H., and Fuller, R.S. (1997). SOI1 Encodes a Novel, Conserved Protein That Promotes TGN–Endosomal Cycling of Kex2p and Other Membrane Proteins by Modulating the Function of Two TGN Localization Signals. J Cell Biol *139*, 23–36.

Burgess, S.M., Delannoy, M., and Jensen, R.E. (1994). MMM1 encodes a mitochondrial outer membrane protein essential for establishing and maintaining the structure of yeast mitochondria. J Cell Biol *126*, 1375–1391.

Chan, D., Frank, S., and Rojo, M. (2006). Mitochondrial dynamics in cell life and death. Cell Death Differ *13*, 680–684.

Cohen, Y., Klug, Y.A., Dimitrov, L., Erez, Z., Chuartzman, S.G., Elinger, D., Yofe, I., Soliman, K., Gärtner, J., Thoms, S., et al. (2014). Peroxisomes are juxtaposed to strategic sites on mitochondria. Molecular BioSystems *10*, 1742.

DiCarlo, J.E., Norville, J.E., Mali, P., Rios, X., Aach, J., and Church, G.M. (2013). Genome engineering in Saccharomyces cerevisiae using CRISPR-Cas systems. Nucl. Acids Res. gkt135.

Dobson-Stone, C., Danek, A., Rampoldi, L., Hardie, R.J., Chalmers, R.M., Wood, N.W., Bohlega, S., Dotti, M.T., Federico, A., Shizuka, M., et al. (2002). Mutational spectrum of

the CHAC gene in patients with chorea-acanthocytosis. European Journal of Human Genetics *10*, 773–781.

Elbaz-Alon, Y., Rosenfeld-Gur, E., Shinder, V., Futerman, A.H., Geiger, T., and Schuldiner, M. (2014). A Dynamic Interface between Vacuoles and Mitochondria in Yeast. Developmental Cell *30*, 95–102.

Freese, E.B., Chu, M.I., and Freese, E. (1982). Initiation of yeast sporulation by partial carbon, nitrogen, or phosphate deprivation. Journal of Bacteriology *149*, 840–851.

Gallagher, P.G. (2004). Hereditary elliptocytosis: spectrin and protein 4.1R. Seminars in Hematology *41*, 142–164.

Hamasaki, M., Furuta, N., Matsuda, A., Nezu, A., Yamamoto, A., Fujita, N., Oomori, H., Noda, T., Haraguchi, T., Hiraoka, Y., et al. (2013). Autophagosomes form at ER-mitochondria contact sites. Nature *495*, 389–393.

Hara, T., Nakamura, K., Matsui, M., Yamamoto, A., Nakahara, Y., Suzuki-Migishima, R., Yokoyama, M., Mishima, K., Saito, I., Okano, H., et al. (2006). Suppression of basal autophagy in neural cells causes neurodegenerative disease in mice. Nature *441*, 885–889.

Hayashi, T., Kishida, M., Nishizawa, Y., Iijima, M., Koriyama, C., Nakamura, M., Sano, A., and Kishida, S. (2012). Subcellular localization and putative role of VPS13A/chorein in dopaminergic neuronal cells. Biochemical and Biophysical Research Communications *419*, 511–516.

Hoppins, S., Collins, S.R., Cassidy-Stone, A., Hummel, E., DeVay, R.M., Lackner, L.L., Westermann, B., Schuldiner, M., Weissman, J.S., and Nunnari, J. (2011). A mitochondrial-focused genetic interaction map reveals a scaffold-like complex required for inner membrane organization in mitochondria. J Cell Biol *195*, 323–340.

Klecker, T., and Westermann, B. (2014). Mitochondria Are Clamped to Vacuoles for Lipid Transport. Developmental Cell *30*, 1–2.

Knop, M., and Strasser, K. (2000). Role of the spindle pole body of yeast in mediating assembly of the prospore membrane during meiosis. The EMBO Journal *19*, 3657–3667.

Kornmann, B. (2013). The molecular hug between the ER and the mitochondria. Current Opinion in Cell Biology *25*, 443–448.

Kornmann, B., Currie, E., Collins, S.R., Schuldiner, M., Nunnari, J., Weissman, J.S., and Walter, P. (2009). An ER-Mitochondria Tethering Complex Revealed by a Synthetic Biology Screen. Science *325*, 477–481.

Kornmann, B., Osman, C., and Walter, P. (2011). The conserved GTPase Gem1 regulates endoplasmic reticulum–mitochondria connections. PNAS *108*, 14151–14156.

Marcusson, E.G., Horazdovsky, B.F., Cereghino, J.L., Gharakhanian, E., and Emr, S.D. (1994). The sorting receptor for yeast vacuolar carboxypeptidase Y is encoded by the VPS10 gene. Cell *77*, 579–586.

Miki, Y., Nishie, M., Ichiba, M., Nakamura, M., Mori, F., Ogawa, M., Kaimori, M., Sano, A., and Wakabayashi, K. (2010). Chorea-acanthocytosis with upper motor neuron degeneration and 3419_3420 delCA and 3970_3973 delAGTC VPS13A mutations. Acta Neuropathologica *119*, 271–273.

Neiman, A.M. (1998). Prospore Membrane Formation Defines a Developmentally Regulated Branch of the Secretory Pathway in Yeast. J Cell Biol *140*, 29–37.

Park, J.-S., and Neiman, A.M. (2012). VPS13 regulates membrane morphogenesis during sporulation in Saccharomyces cerevisiae. J Cell Sci *125*, 3004–3011.

Park, J.-S., Okumura, Y., Tachikawa, H., and Neiman, A.M. (2013). SPO71 Encodes a Developmental Stage-Specific Partner for Vps13 in Saccharomyces cerevisiae. Eukaryotic Cell *12*, 1530–1537.

Parodi, E.M., Baker, C.S., Tetzlaff, C., Villahermosa, S., and Huang, L.S. (2012). SPO71 Mediates Prospore Membrane Size and Maturation in Saccharomyces cerevisiae. Eukaryotic Cell *11*, 1191–1200.

Pfeffer, S.R. (2001). Membrane transport: Retromer to the rescue. Current Biology *11*, R109–R111.

Rabitsch, K.P., Tóth, A., Gálová, M., Schleiffer, A., Schaffner, G., Aigner, E., Rupp, C., Penkner, A.M., Moreno-Borchart, A.C., Primig, M., et al. (2001). A screen for genes required for meiosis and spore formation based on whole-genome expression. Current Biology *11*, 1001–1009.

Rampoldi, L., Dobson-Stone, C., Rubio, J.P., Danek, A., Chalmers, R.M., Wood, N.W., Verellen, C., Ferrer, X., Malandrini, A., Fabrizi, G.M., et al. (2001). A conserved sorting-associated protein is mutant in chorea-acanthocytosis. Nature Genetics *28*, 119–120.

Rizzuto, R., Duchen, M.R., and Pozzan, T. (2004). Flirting in Little Space: The ER/Mitochondria Ca2+ Liaison. Sci. Signal. *2004*, re1–re1.

Robinson, J.S., Klionsky, D.J., Banta, L.M., and Emr, S.D. (1988). Protein sorting in Saccharomyces cerevisiae: isolation of mutants defective in the delivery and processing of multiple vacuolar hydrolases. Mol. Cell. Biol. *8*, 4936–4948.

Rose, M.D., and Fink, G.R. (1990). Methods in Yeast Genetics (Cold Spring Harbor, NY: Cold Spring Harbor Laboratory Press).

Salomao, M., Zhang, X., Yang, Y., Lee, S., Hartwig, J.H., Chasis, J.A., Mohandas, N., and An, X. (2008). Protein 4.1R-dependent multiprotein complex: New insights into the structural organization of the red blood cell membrane. PNAS *105*, 8026–8031.

Stevens, T., Esmon, B., and Schekman, R. (1982). Early stages in the yeast secretory pathway are required for transport of carboxypeptidase Y to the vacuole. Cell *30*, 439–448.

Tomiyasu, A., Nakamura, M., Ichiba, M., Ueno, S., Saiki, S., Morimoto, M., Kobal, J., Kageyama, Y., Inui, T., Wakabayashi, K., et al. (2011). Novel pathogenic mutations and copy number variations in the VPS13A Gene in patients with chorea-acanthocytosis. American Journal of Medical Genetics Part B: Neuropsychiatric Genetics *156*, 620–631.

Velayos-Baeza, A., Vettori, A., Copley, R.R., Dobson-Stone, C., and Monaco, A.P. (2004). Analysis of the human VPS13 gene family. Genomics *84*, 536–549.

Wideman, J.G., Go, N.E., Klein, A., Redmond, E., Lackey, S.W.K., Tao, T., Kalbacher, H., Rapaport, D., Neupert, W., and Nargang, F.E. (2010). Roles of the Mdm10, Tom7, Mdm12, and Mmm1 Proteins in the Assembly of Mitochondrial Outer Membrane Proteins in Neurospora crassa. Mol. Biol. Cell *21*, 1725–1736.

Yamano, K., Tanaka-Yamano, S., and Endo, T. (2010). Mdm10 as a dynamic constituent of the TOB/SAM complex directs coordinated assembly of Tom40. EMBO Reports *11*, 187–193.

Zimprich, A., Benet-Pagès, A., Struhal, W., Graf, E., Eck, S.H., Offman, M.N., Haubenberger, D., Spielberger, S., Schulte, E.C., Lichtner, P., et al. (2011). A Mutation in VPS35, Encoding a Subunit of the Retromer Complex, Causes Late-Onset Parkinson Disease. The American Journal of Human Genetics *89*, 168–175.